Review

Natural Alkaloids and Heterocycles as G-Quadruplex Ligands and Potential Anticancer Agents

Tong Che, Yu-Qing Wang, Zhou-Li Huang, Jia-Heng Tan, Zhi-Shu Huang and Shuo-Bin Chen *

School of Pharmaceutical Sciences, Sun Yat-sen University, Guangzhou 510006, China;
chetong@mail2.sysu.edu.cn (T.C.); wangyuq2@mail2.sysu.edu.cn (Y.-Q.W.);
huangzhli@mail2.sysu.edu.cn (Z.-L.H.); tanjiah@mail.sysu.edu.cn (J.-H.T.); ceshzs@mail.sysu.edu.cn (Z.-S.H.)
* Correspondence: chenshb8@mail.sysu.edu.cn; Tel.: +86-20-3994-3072

Abstract: G-quadruplexes are four-stranded nucleic acid secondary structures that are formed in guanine-rich sequences. G-quadruplexes are widely distributed in functional regions of the human genome and transcriptome, such as human telomeres, oncogene promoter regions, replication initiation sites, and untranslated regions. Many G-quadruplex-forming sequences are found to be associated with cancer, and thus, these non-canonical nucleic acid structures are considered to be attractive molecular targets for cancer therapeutics with novel mechanisms of action. In this mini review, we summarize recent advances made by our lab in the study of G-quadruplex-targeted natural alkaloids and their derivatives toward the development of potential anticancer agents.

1. Introduction

Guanine-rich nucleic acid sequences are able to fold into four-stranded secondary structures known as G-quadruplexes, which arise from the self-association of guanine bases by Hoogsteen hydrogen bonding [1]. Putative quadruplex sequences (PQS) are widespread throughout the human genome, especially at telomeres and regulatory regions of oncogenes [2–4]. G-quadruplexes are now thought to play important roles in several biological events associated with cancer, particularly in telomere maintenance and the expression of oncogenes, and have received much attention [5–8]. The conformations of G-quadruplexes provide recognition sites for small molecules, and thus, these structures are promising targets for the design of anticancer drugs [9,10].

Although there remains a long way to go in the development of potent drugs that target G-quadruplexes, some promising lead compounds have been obtained. For example, telomestatin, which selectively binds to telomeric G-quadruplex DNA, was able to cause telomere dysfunction by inhibiting telomerase activity and disturbing the sheltering complex [11,12]. Pyridostatin (PDS) could inhibit the transcription of G-quadruplex-related genes while interacting with promoter G-quadruplexes [13]. Notably, the ribosomal DNA (rDNA) G-quadruplex ligand Quarfloxin (CX-3543), which was able to disrupt nucleolin/rDNA G-quadruplex complexes and block the biogenesis of rRNA, has once enter the phase II clinical trials [14]. There is large evidence that ligands which can stabilize G-quadruplex are able to interfere with the G-quadruplex related biological events associated with cancer [15].

Some of these reported G-quadruplex ligands are natural alkaloids [16,17], which are an important class of natural products that have diverse and significant biological activities, such as antimalarial and anticancer activities. Because these compounds exhibit chemical diversity and structural complexity and are available from natural sources, natural alkaloids and their derivatives, such as telomestatin, the quindoline derivative CX-3543, the bis-quinoline derivative PDS and the acridine derivative BRACO-19, have been investigated intensively for their potential as G-quadruplex ligands [18–20].

In this paper, we summarize the previously published research from our lab on G-quadruplex-targeting natural alkaloids and heterocycles as potential anticancer agents.

2. G-Quadruplex Structures

Guanine-rich strands have high propensity to self-associate into unusual structures called G-quadruplexes (Figure 1), which were first reported by Davies and co-workers in 1962 [21]. G-quadruplex topology is clearly different from that of B-DNA and other types of DNA. The basic building block of a G-quadruplex is a structure in which four guanine residues form a ring-like, aromatic, planar G-tetrad structure via Hoogsteen hydrogen bonds between the N1, N7, O6 and N2 sites. With the advent of X-ray crystallography, nuclear magnetic resonance spectroscopy (NMR) and other powerful technologies, the structures of many G-quadruplexes have been resolved [22,23]. G-quadruplex structures can fold due to either intra- or intermolecular interactions of G-rich strands. Structural polymorphism arises mostly from the properties of the loop, such as variations in strand stoichiometry, strand polarity, and glycosidic torsion angle and the sites on the loop that link to the guanine strand [24]. Moreover, the solution conditions, such as the presence of metal ions or ligands, or molecular crowding, may also influence the topology of quadruplexes. G-quadruplexes can form via intramolecular folding of a single G-rich sequence or by intermolecular association of two (dimeric) or four (tetrameric) separate strands. The relative arrangement of strand polarity can also give rise to structural polymorphism. For example, the polarities of the four strands in a G-quadruplex can be arranged as follows: all parallel strands; three parallel strands and one antiparallel strand; adjacent parallel strands; or alternating parallel strands. These arrangements lead to different conformations, namely, parallel, propeller, and antiparallel quadruplexes [25,26]. The conformations of G-quadruplexes formed from the folding of different G-rich sequences are distinct. G-quartet regions, loop regions, groove dimensions, and the negative electrostatic potential of the anionic backbone and the central channel of G-quadruplexes are critical elements that need to be considered in order to improve the binding selectivity of drug candidates [12,27–29].
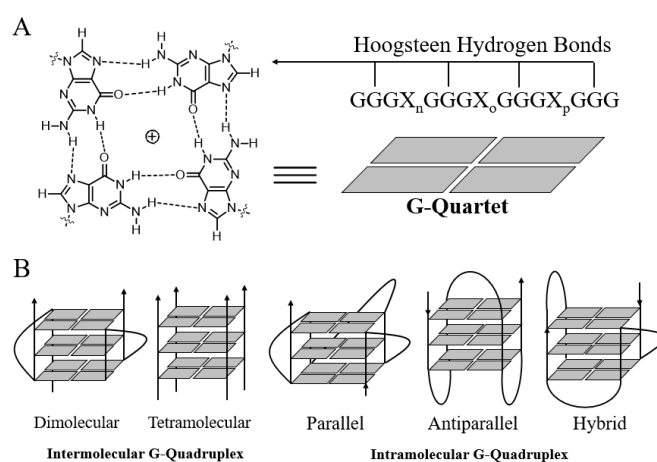
Figure 1. Structures of the G-quartet (**A**) and G-quadruplexes (**B**).

3. Existence and Distribution of G-Quadruplexes

Computational predictions using simple algorithms suggest that over 370,000 sequence motifs (of the type $G_{\geq 3}N_{1–7}G_{\geq 3}N_{1–7}G_{\geq 3}N_{1–7}G_{\geq 3}$) in the human genome have the potential to form G-quadruplex structures [2]. These PQSs are frequently found within human telomeric DNA, rDNA, transcription start sites, and promoter regions, suggesting that G-quadruplex structures may play a pivotal role in the regulation of a variety of cellular processes, including telomere maintenance, ribosome biogenesis, gene replication and transcription [3]. A method that combines G-quadruplex-dependent DNA polymerase stalling and next-generation sequencing (G4-seq) has been

developed and was used to obtain a genome-wide map of G-quadruplex structures in purified, single-stranded human DNA. G4-seq has identified more than 700,000 G-quadruplexes in the human genome, which is much higher than the values predicted by earlier algorithms. A majority (70%) of these sequences either comprise G-tracts that are interrupted by non-guanine sequences and are predicted to form bulges or comprise extra-long loops [4]. Another method, which couples reverse transcriptase stalling with next-generation sequencing (rG4-seq), was developed and was used to characterize more than 13,000 G-quadruplexes in the human transcriptome. The enrichment of G-quadruplexes in transcripts that mediate RNA processing and stability reveals that RNA G-quadruplexes may play roles in the regulation of transcripts via miRNA-mediated gene regulation and alternative polyadenylation [7]. On the other hand, ~10,000 G-quadruplexes were identified in human chromatin by an antibody-based G-quadruplex chromatin immunoprecipitation and high-throughput sequencing approach (G4 ChIP-seq); these G-quadruplexes were identified predominantly in regulatory, nucleosome-depleted regions [5]. G-quadruplex structures are enriched in the promoters and 5′ UTRs of highly transcribed genes, particularly in genes related to cancer, and in somatic copy number alterations (SCNAs). The findings of G-quadruplex-related sequencing suggest that the variety and number of potential G-quadruplexes are greater than originally predicted.

Studies involving the visualization of G-quadruplexes by antibodies and small-molecule probes have provided crucial evidence of the existence of G-quadruplexes in cells [30]. Schaffitzel et al., who were the first to report the visualization of G-quadruplex formation in a biologically relevant context, used a G-quadruplex-selective antibody, Sty49, to show that G-quadruplexes form at telomeres in the macronuclei of the ciliate *Stylonychia lemnae* [31]. DNA G-quadruplexes were then observed at the ends of human chromosomes by using the radiolabeled ligand ^{3}H-360A and the fluorescent ligand BMVC [32,33]. Subsequently, DNA G-quadruplexes were visualized in the nuclei of human cells by in situ fluorescence labelling of PDS and immunofluorescence microscopy using the G-quadruplex-specific antibody BG4 [13,34]. Notably, the number of BG4 foci increased after the exposure of live cells to G-quadruplex ligands, including PDS, Phen-DC3 and TMPyP4, which demonstrates that these ligands trap the G-quadruplex structures formed in cells. Furthermore, interactions between small molecules and DNA G-quadruplexes were visualized in live cells by fluorescence-lifetime imaging microscopy using DAOTA-M2. Several fluorescent probes capable of discriminating DNA G-quadruplexes from single- and double-stranded nucleic acids have also been described previously [35–39]. Compared with the detection of DNA quadruplexes, the detection of cellular RNA quadruplexes was more challenging. RNA quadruplexes were first detected by immunodetection using BG4 in 2014 [40]. This finding provides substantive evidence for the existence of RNA G-quadruplexes in human cells. On the other hand, this investigation also demonstrates that the ligand carboxyPDS, which binds to G-quadruplexes in vitro, can trap endogenous RNA G-quadruplexes when used in cells. This result corroborates the results obtained by using stabilizing ligands that target G-quadruplexes in a cellular context. RNA G-quadruplexes were then observed in live cells by using the multiphoton turn-on fluorescent probe NaphthoTASQ in 2015 [41]. More recently, a G-quadruplex-triggered fluorogenic hybridization (GTFH) probe reported by our research group specifically visualized the RNA G-quadruplex structure formed by the G-rich sequence within the 5′-UTR of NRAS mRNA in the cytoplasm of human cells [42]. Overall, antibodies and fluorescent probes capable of structure-specific detection of G-quadruplexes are powerful tools for basic biological research and for the exploration of G-quadruplexes as a potential drug targets.

4. G-Quadruplexes as Promising Targets for Anticancer Drug Design

4.1. Telomeric G-Quadruplexes

Human telomeres comprise tandem repeats of the DNA motif TTAGGG together with associated telomeric proteins and feature a 50–300-nucleotide protrusions of single-stranded repeats from the 3′ end, termed the G-tail or G-overhang [43]. This G-overhang acts as a substrate for telomerase,

a reverse transcriptase with an RNA component that is required for telomere extension. The structure and stability of telomeres are closely related to cancer, aging, and genetic stability. Due to the high frequency of TTAGGG repeats and due to the lack of competition from a complementary strand at the 3′ overhang, the formation of a G-quadruplex would be favored.

The formation of a G-quadruplex can affect telomeres in profound ways, including (a) inhibiting telomerase activity by blocking the binding of telomerase to the single-stranded telomere substrate to elongate the telomeres. Telomerase is overexpressed in 80–85% of cancer cells and primary tumors, making it an attractive target for cancer therapeutics [44]; (b) telomere uncapping by dissociation of telomere-binding proteins (e.g., POT1, TRF1 and TRF2) from the end of the telomere. Telomere uncapping can lead to telomeric dysfunction, which is characterized by end-to-end fusion, inappropriate recombination, anaphase bridges, and G-overhang degradation, and leads to either apoptosis or senescence [45]; and (c) interfering with telomere replication by impairing replication fork progression. These findings prompted the development of several selective G-quadruplex-binding small molecules with the aim of developing novel telomere-based anticancer therapies.

Recently, a number of studies showed that the 3′-terminal single-stranded overhang could form several consecutive quadruplex units connected by TTA linkers, called telomeric multimeric G-quadruplexes [46–49]. This distinctive structure enables the possibility of designing small molecules that are able to discriminate telomeric G-quadruplexes from a large number of other G-quadruplexes with various biological functions [50]. Thus, it has been suggested that small molecules that specifically target telomeric multimeric G-quadruplexes might be more promising as anticancer agents and might have fewer side effects.

4.2. Oncogene Promoter Region G-Quadruplexes

In addition to telomeric G-quadruplexes, several putative G-quadruplex sequences have been identified near transcription start sites and gene promoters, indicating the key role of these structures in the regulation of various genes. These gene promoters include the promoters of c-MYC, c-KIT, bcl-2, K-RAS, VEGF, RB, PDGF-A, hTERT [51–58]. More importantly, altered expression of these oncogenes are recognized as hallmarks of cancer. At the turn of the century, Hanahan and Weinberg proposed six vital cellular and microenvironmental processes that are aberrantly regulated during oncogenic transformation and malignancy [59]. When each of these categories is examined, one or more critical proteins are found to have G-quadruplexes in the core or proximal promoter regions. Transcriptional repression of oncogenes by stabilization of G-quadruplex structures or by inhibiting the binding of related proteins to these structures could be a novel anticancer strategy.

c-MYC is one of the best-studied oncogenes. Up to 80% of all solid tumors, including gastrointestinal, ovarian and breast cancer tumors, overexpress c-MYC as do many non-Hodgkin's lymphoma tumors [60]. The nuclease-hypersensitive element (NHE III$_1$) in the c-MYC promoter regulates 85–90% of c-MYC transcription. The region contains 27 guanine-rich bases (referred to as Pu27 herein) that can fold into a G-quadruplex that is considered a transcription repressor element. Several G-quadruplex-binding ligands possess the ability to promote and/or stabilize the c-MYC G-quadruplex structure, thus repressing c-MYC transcription [51]. Generally, gene transcription is triggered and regulated by transcription factors. Transcription factors promote or repress gene transcription by recognizing and binding to certain regions in promoters and then recruiting other factors. In most cancer cells, the expression of transcription factors is usually abnormal, which theoretically makes these proteins promising targets for the development of anticancer drugs.

4.3. RNA G-Quadruplexes

There is emerging evidence that 5′- and 3′-untranslated regions as well as open reading frames (ORFs) contain putative RNA G-quadruplexes. Due to the absence of a complementary strand in RNA molecules, it has been widely held that G-rich RNA sequences are more susceptible to the formation of G-quadruplex structures. Unlike the highly polymorphic DNA G-quadruplex structures

that depend on the surrounding conditions, RNA G-quadruplexes almost exclusively adopt a single conformation. The presence of a 2′-hydroxyl group in the ribose sugar results in additional steric constraints on the G-quadruplex topology. These 2′-hydroxyl groups prevent the base from adopting a syn-conformation, instead strongly favoring the anti-conformation (by restraining the glycosidic torsion angle) and imposing additional constraints on sugar puckering (ribose has a preference for C3′-endo puckering). As a consequence, the topology of RNA G-quadruplexes is limited to the parallel conformation, in which all four strands are oriented in the same direction. There is ample evidence that RNA G-quadruplexes exist in the UTRs and ORFs of cancer-related genes that regulate transcription, alternative splicing and translation. In addition, the unique chemical properties of RNA G-quadruplexes suggest that it is possible to develop small molecules that selectively bind to RNA G-quadruplexes rather than DNA G-quadruplexes. This preferential binding is exemplified by the small molecule carboxyPDS, which exhibits high molecular specificity for RNA G-quadruplexes over DNA G-quadruplexes. Selective intervention by targeting only RNA G-quadruplexes may be a strategically important therapeutic approach for cancer.

Recently, a high-throughput method was developed that identifies RNA G-quadruplex regions on the basis of the propensity of the RNA to stall reverse transcriptase in a K^+-dependent manner. By applying this method to RNA from mammalian cell lines and yeast, >10,000 endogenous regions that form RNA G-quadruplexes in vitro were identified, thereby expanding the catalog of endogenous regions with experimentally confirmed propensity to fold into RNA G-quadruplex structures by a factor of >100. To determine the folding state of these RNA G-quadruplex regions in vitro and in cells, dimethyl sulfate (DMS) treatment was performed before mapping the reverse transcriptase stops. The results showed that, in contrast to previous assumptions, regions that folded into RNA G-quadruplex structures in vitro were overwhelmingly unfolded in eukaryotic cells [61]. Taken together, various independent studies on RNA G-quadruplexes reveal promising regulatory functions of these structures in multiple biological processes. However, these challenging puzzles have only been partially solved, and comprehensive studies should be undertaken to understand the behavior of RNA G-quadruplexes, such as the folding dynamics, stability and biological relevance in vivo and the detailed mechanism of RNA G-quadruplexes involved in regulatory processes.

5. Natural Alkaloids and Their Derivatives as G-Quadruplex Ligands

### 5.1. Methods to Discover G-Quadruplex Ligands

As mentioned above, G-quadruplexes play important roles in several biological events associated with cancer. Selective intervention by targeting G-quadruplexes may be a strategically important therapeutic approach for cancer. Thus, the discovery of potential G-quadruplex was important. Generally, a good G4 ligand binds G-quadruplex with strong potency and selectivity over duplex and other nucleic acid structures in vitro. While in vivo, they are potent to interfere G4-involved biological events, such as the telomere maintenance and gene expression. Various methods, including those in vitro, in cells and in silicon, have been developed and applied in the screen of G-quadruplex ligands. Several frequently used G-quadruplex ligand screening methods are summarized in Table 1. Besides, optimization based on these known G-quadruplex interactive moieties is emerging as an effective approach to develop new G-quadruplex ligands, which will be elaborated in the following parts.

Table 1. Methods for the discovery of G-quadruplex ligands.

Methods	Screening Index	Ref.
3D-QSAR Pharmacophore	Chemical feature of active compounds	[62]
Molecular docking	Estimated binding affinity to G-quadruplex	[63]
Fluorescence displacement (FID)	Competed binding towards G-quadruplex	[64]
NMR	Binding site with G-quadruplex	[65]
Fluorescence resonance energy transfer (FRET)	Stability effect of compounds on G-quadruplex	[66]
Surface plasmon resonance (SPR)	Binding affinity to G-quadruplex	[67]
G-quadruplex on Oligo Affinity Support (G4-OAS)	Binding affinity to G-quadruplex	[68]

5.2. Quindoline Derivatives

Quindoline (**1**, Figure 2) is a naturally occurring indolo[3,2-*b*]quinoline alkaloid. Quindoline was originally synthesized in 1906 and has since been prepared from cryptolepine (**2**). Quindoline was first extracted from the African plant *Cryptolepis sanguinolenta* (Periplocaceae) in 1978. This compound has antimicrobial, antimalarial, anti-inflammatory, and antihypolipidemic activities. In 2000, Neidle et al. first reported that the 2,10-disubstituted quindoline derivative **3** could bind to G-quadruplex structures in human telomeres, showing it to have modest cytotoxicity against several cancer cells as well as inhibitory activity against telomerase, with an IC_{50} ($^{tel}IC_{50}$) of 16 µM [69]. They further determined that the 2,7-disubstituted quindoline derivative **4** showed more potent activity than **3**, with a $^{tel}IC_{50}$ value of 6.3 µM [70].
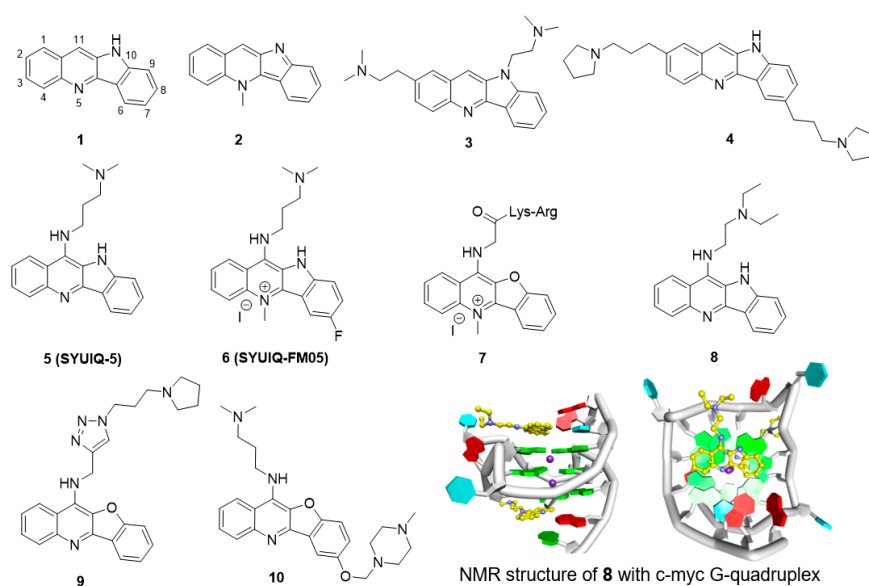
Figure 2. Structures of quindoline derivatives and binding mode with G-quadruplex.

The 11-substituted quindoline derivatives designed and synthesized by our research group exhibited significantly improved ability to stabilize telomeric G-quadruplexes [71,72]. The introduction of electron donating groups at position 11 enhances the basicity of the nitrogen atom in the pyridine ring, thus enhancing the electrostatic interaction between the derivatives and the negative electrostatic center of the G-quadruplex. The most active derivative, **5** (SYUIQ-5), showed improved inhibition of telomerase activity ($^{tel}IC_{50}$ = 0.44 µM) and induced a marked cessation in cell growth and a cellular senescence phenotype in human leukemia K562 cells and colon cancer SW620 cells [73]. The growth cessation was accompanied by a shortening of telomere length and upregulation of the expression of the cyclin-dependent kinase inhibitors p16, p21 and p27.

Further studies on SYUIQ-5 indicated that the 11-alkylamino group on quindoline could lead to in situ protonation of the 5-*N* atom [74]. Molecular modeling studies revealed that the crescent-shaped aromatic core was stacked on two guanine residues of the G-quartet, and the 5-*N* electropositive center overlapped with the cation channel of the quadruplex. However, the pKa values of the 5-*N* atoms of the 11-aminoquinolines were 8.2–8.4 and thus could be easily influenced by the conditions in the solution. An alternative to the introduction of a positive charge via in situ protonation was *N*-methylation at the 5-position. Based on this hypothesis, a series of 5-*N*-methyl quindoline derivatives were designed for screening ligands with better binding ability and that selectively recognized telomeric G-quadruplexes. The results showed that the 5-*N*-methyl quindoline derivatives not only exhibited significantly higher binding affinity for G-quadruplexes (approximately 5-fold higher than the non-methylated derivatives) but also exhibited selectivity toward antiparallel telomeric quadruplexes. Derivative **6** markedly

inhibited telomerase activity in a cell-free system ($^{tel}IC_{50}$ = 0.31 μM). The determination of short-term cell viability by a two-day cytotoxicity assay (MTT assay) showed that **6** had a potent inhibitory effect on leukemia HL60 cells and lymphoma CA46 cells. Long-term exposure of HL60 and CA46 cells to **6** induced marked cessation of population growth, a cellular senescence phenotype, and shortening of telomere length.

Quindoline derivatives were capable of interacting with the telomeric G-quadruplex structure and exhibited inhibition of telomerase activity. However, studies showed that cryptolepine could interact with the CC sites of the DNA fragment d(CCTAGG)$_2$ in a base-stacking intercalation mode. Thus, further studies were undertaken to improve the selectivity of these compounds. It has been reported that a combination of peptides that selectively bind to DNA scaffolds would greatly increase the selectivity of these peptides for G-quadruplexes versus duplex DNA. A series of peptidyl-benzofuroquinoline conjugates were designed and synthesized. The positive charge and alkyl-chain length of the dipeptidyl side chain proved to be important for the interaction of the side chain with the G-quadruplex. Derivative **7**, with a -Lys-Arg dipeptide fragment, exhibited the most potent telomerase inhibition ($^{tel}IC_{50}$ = 5.5 μM) and had 50 times higher selectivity for telomeric G-quadruplex than for the duplex. Additionally, cellular experiments also showed a marked cessation in population growth and a cellular senescence phenotype as well as shortening of the telomere length [75].

In addition to telomeric single-stranded overhangs, G-quadruplexes are also present in the promoter or regulatory regions of important oncogenes such as c-MYC, BCL-2 and c-KIT. c-MYC is an important proto-oncogene, and the aberrant overexpression of this gene is always associated with a variety of malignant tumors. Further studies have shown that SYUIQ-5 can also interact with the c-MYC G-quadruplex and inhibit the expression of this gene. A PCR stop assay showed that in the presence of SYUIQ-5, the Pu22 c-MYC oligomer was induced to form a G-quadruplex, which prevented hybridization with a complementary strand that overlapped with the last G repeat. The expression of c-MYC was seen to be markedly inhibited when the mRNA and protein levels in HL-60 and K562 cells were measured. Derivative **8**, with a short side chain, showed more potential stabilization of the c-MYC G-quadruplex. Further studies showed that **8** could inhibit the expression of c-MYC in the hepatocellular carcinoma cell line Hep G2. The binding of derivative **8** with c-MYC G-quadruplex was explored by Yang et al. [76]. Structural NMR results showed quindoline could stack effectively on both sides of G-quadruplex, and unexpectedly, the structure showed that the quindoline-induced reorientation of the flanking sequences led to the formation of a new binding pocket (Figure 2).

The quindoline derivatives were seen to interact with the G-quadruplex in the c-MYC gene with a certain degree of selectivity, and the specificities were further improved. The heteroaromatic 1,4-substituted 1,2,3-triazole ring system has attracted extensive interest in drug design owing to the wide applicability of this system as a synthetic building block endowed with pharmacological potential. A series of novel triazole-containing benzofuroquinoline derivatives (T-BFQs) were designed and synthesized by 1,3-dipolar cycloaddition of a series of alkyne and azide building blocks [77]. The selectivity of these novel T-BFQs toward c-MYC G-quadruplex DNA was significantly improved, and a distinct increase in binding affinity was observed. Further cellular experiments showed that derivative **9** specifically downregulated c-MYC gene transcription and expression in RAJI cells. Derivative **9** exhibited inhibition of tumor cell proliferation but had a weak effect on primary cultured mouse mesangial cells (in which proliferation does not depend on c-MYC expression). These results indicated that inhibition by **9** presumably occurs via the downregulation of transcription of the c-MYC gene. Tumor-bearing mice treated with derivative **9** had an average tumor volume of <400 mm^3 and exhibited an inhibition rate of 38.1% (Table 2).

Recently, four series of 7,11-disubstituted quindoline derivatives were also synthesized by introducing a second cationic amino side chain and a 5-*N*-methyl group as ligands to bind to the c-MYC promoter G-quadruplex. In vitro evaluations showed that the derivates exhibited increased stabilities and binding affinities, and most of the derivatives had better selectivity for the c-MYC G-quadruplex (over duplex DNA) compared to SYUIQ-5. Moreover, the new derivatives prevented

NM23-H2, a transcription factor, from effectively binding to the c-MYC G-quadruplex. Further studies showed that derivative **10** downregulated c-MYC transcription by targeting the promoter G-quadruplex and disrupting the NM23-H2/c-MYC interaction in RAJI cells. Derivative **10** could inhibit Burkitt's lymphoma cell proliferation through cell cycle arrest and apoptosis and suppress tumor growth in a human Burkitt's lymphoma xenograft with an inhibition rate of 27.4% (Table 2) [78].

Table 2. Anti-tumor activity of alkaloid derivatives in vivo.

Derivatives	Xenograft Model	Dosage $(mg \cdot kg^{-1})$	Tumor Growth Inhibition	Days to Complete Response	Ref.
9	A549 human lung cancer	6.25; i.p.	38.1%	12	[77]
10	RAJI human Burkitt's lymphoma	30; i.p.	27.4%	14	[78]
15	SiHa human cervical squamous cancer	20; i.p.	35.2%	20	[79]
16		5; i.p.	64.8%	21	[79]
21		1; i.p.	49.3%	20	[79]
24	MCF-7 human breast cancer	7.5; i.p.	60.1%	20	[79]

5.3. Isaindigotone Derivatives

Isaindigotone (**11**, Figure 3) is an alkaloid isolated from the root of the traditional Chinese herb *Isatis indigotica* Fort [80]. This compound exhibits excellent effects against influenza, epidemic hepatitis, and epidemic encephalitis. The structure of isaindigotone comprises a pyrrolo[2,1-*b*]quinazoline moiety conjugated with a benzylidene group. Our group first synthesized a series of isaindigotone derivatives to explore the effects of the derivatives on G-quadruplex stability and selectivity [81–83]. The unfused aromatic rings and tethered side chains of these derivatives seemed to allow the compounds to adopt flexible and adaptive conformations, which help in the recognition of telomeric G-quadruplex cores and grooves in a 4:1 binding mode. Derivative **12** significantly induced cell senescence and telomere shortening of HL-60 cells and CA46 cells at micromolar concentrations. A TRAP-LIG assay showed that derivative **12** inhibited telomerase activity with an $^{tel}IC_{50}$ value of 7.8 μM. To better investigate how the planarity of an unfused aromatic ligand impacts the quadruplex-binding properties of the ligand, another series of isaindigotone derivatives were designed and were reported to stabilize the c-KIT G-quadruplex. The best derivative, **13**, reduced the transcription of c-KIT by 52.5% and exhibited significant cytotoxicity in a gastrointestinal stromal tumor cell line. SAR analysis showed that expansion of the aromatic system via the introduction of a benzene ring, a benzylidene group and two cationic amino side chains into the quinazolone moiety not only maximizes the stacking interactions of the derivatives with the G-quartet but also incorporates features of flexibility that prevent the derivative from intercalating with duplex DNA.
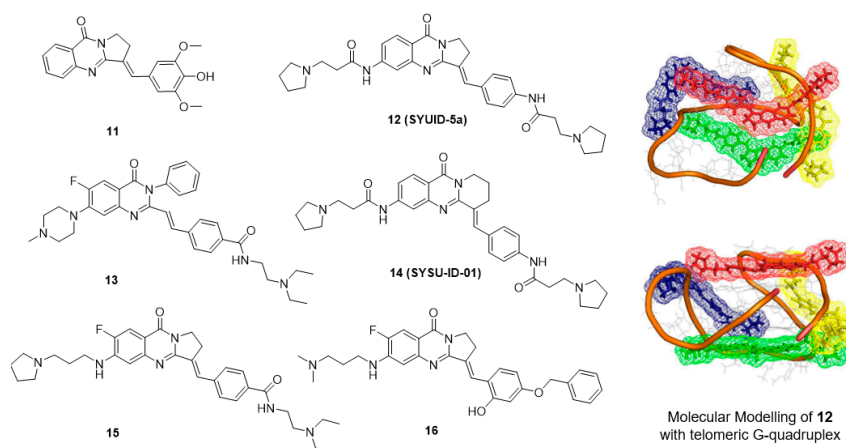
**Figure 3.** Structures of isaindigotone derivatives and binding mode with G-quadruplex.

Currently, a number of small molecule ligands that stabilize G-quadruplexes have been developed [84,85]. However, selectively targeting a specific G-quadruplex is still a difficult task [86,87]. Typically, the interaction between protein and DNA is highly specific and stable. By targeting the interaction of a G-quadruplex-related protein with the G-quadruplex, new opportunities are emerging for the development of small molecules that target G-quadruplexes. In the process of c-MYC transcription, one of the transcription factors, NM23-H2, has an important role in transcriptional reactivation. Studies have revealed that NM23-H2 can recognize and bind to the c-MYC NHE III_1 region and act as an unwinding protein on the G-quadruplex [88]. Therefore, the interaction of NM23-H2 with the c-MYC G-quadruplex might be a key process in the transcriptional regulation of the c-MYC gene, and derivatives that can interfere with the binding of NM23-H2 to the c-MYC G-quadruplex are expected to repress c-MYC transcription. An in-house small-molecule library screening by SPR identified the isaindigotone derivative **14** (SYSU-ID-01), which significantly interfered with the binding of NM23-H2 to the c-MYC promoter DNA [79]. Further analyses of the derivative-protein interaction and the protein-DNA interaction provided insight into the mode of action of SYSU-ID-01. Results of cellular evaluation showed that SYSU-ID-01 could abrogate the binding of NM23-H2 to the c-MYC promoter, resulting in downregulation of c-MYC transcription and dramatically suppressed HeLa cell growth. However, in primary cultured mouse mesangial cells, in which proliferation does not depend on c-MYC expression, instead of proliferation arrest, SYSU-ID-01 promoted cell proliferation.

These results inspired further modification, and a series of new isaindigotone derivatives were designed and synthesized [89,90]. The abilities of these derivatives to interact with G-quadruplexes or with NM23-H2 and to disrupt the G-quadruplex-NM23-H2 interaction were evaluated. Among these derivatives, derivative **15** showed marked disruption of the G-quadruplex-NM23-H2 interaction. This compound exhibited significant effects on c-MYC-related processes in SiHa cells, including inhibition of transcription and translation, inhibition of cell proliferation, induction of apoptosis, and regulation of the cell cycle. In contrast, derivative **15** promoted cellular growth instead of proliferation arrest in primary cultured mouse mesangial cells. A SiHa xenograft mouse model of human cervical squamous cancer showed that after 3 weeks of treatment, compared with the vehicle group, treatment with derivative **15** at 20 mg/kg resulted in a statistically significant reduction in tumor weight, with a tumor growth inhibition rate of 35.2% (Table 2). Furthermore, to design and synthesize highly specific NM23-H2-binding ligands, the G-quadruplex-ligand features of the derivatives were removed, and only one positive amino side chain remained at the 6-position. A series of novel isaindigotone derivatives with a variety of substituents, such as alkyl, hydroxyl, alkoxy, alkamino, fluoro, and trifluoromethyl groups, at the 4′-position of the styrene ring were designed and synthesized and screened for NM23-H2-selective binding of ligands. Among these derivatives, derivative **16** exhibited significant binding affinity toward NM23-H2 and disrupted the NM23-H2/c-MYC G-quadruplex interaction in vitro and in cells. Inhibition of the transcription of the oncogene c-MYC by **16** induced cell-cycle G0/G1-phase arrest, cellular apoptosis, proliferation inhibition, and migration inhibition. In addition, **16** exhibited potent antiproliferation activity in several cancer cell lines and exhibited good antitumor activity by inhibiting the growth of cervical squamous cancer in BALB/C-nu/nu mice with a SiHa xenograft, with a tumor growth inhibition rate of 64.8% (Table 2).

5.4. Berberine Derivatives

Berberine (**17**) is an alkaloid isolated from Chinese herbs that has long been used as an antimicrobial agent, and this compound has attracted a lot of attention for its antineoplastic effects. Berberine appears to suppress the growth of a variety of tumor cells, including breast cancer, leukemia, prostate carcinoma, and gastric carcinoma cells. In 1999, Tsuruo and coworkers were the first to report that berberine inhibits telomerase activity, thus interrupting telomere elongation [91]. The 13-substituted berberine derivative, **18,** then shows weak binding with telomeric G-quadruplex DNA and poor telomerase inhibition, while 9-*O*-subtituted berberine derivatives, by introducing a

side chain with terminal amino group outside of the crescent-shaped ring system, show significantly improved ability to stabilize telomeric G-quadruplexes [92–94]. A recent X-ray structure of provided an important clue for interpreting data regarding the binding of berberine with telomeric G-quadruplex. The result showed that two berberine molecules could simultaneously interacting with each external G-tetrad via π-stacking, while the crescent-shaped ring of berberine stack over two guanines (Figure 4) [95].
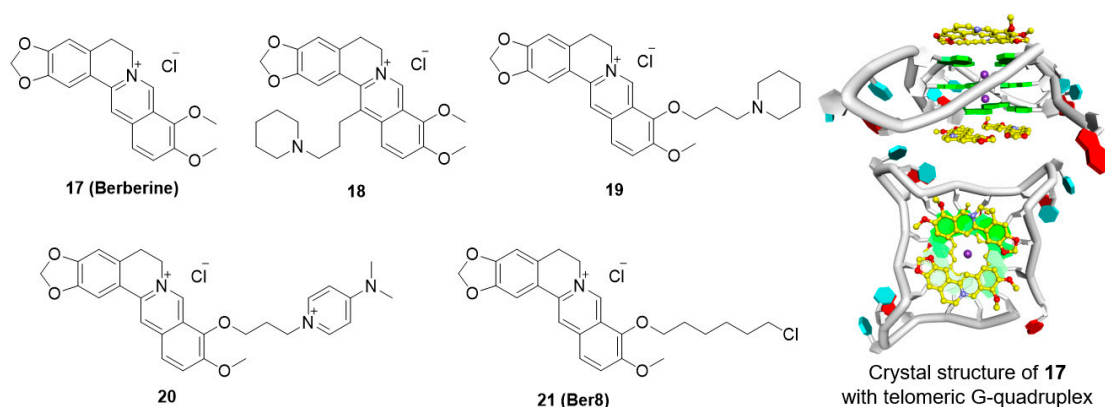
Figure 4. Structures of berberine derivatives and binding mode with G-quadruplex.

Among these derivatives, derivative **19** markedly inhibited telomerase activity, with a $^{tel}IC_{50}$ value of 16 μM. Introduction of a positively charged terminal aza-aromatic group may enhance the electrostatic interaction of the derivative with the phosphate backbone and improve the interaction with the loop region via π-π stacking. Derivative **20,** which had an aza-aromatic group, could selectively bind to telomeric G-quadruplexes over duplex DNA. Derivative **20** had a $^{tel}IC_{50}$ value of 14 μM, which is much lower than that of berberine ($^{tel}IC_{50}$ = 70 μM). Recently, a newly synthesized berberine derivative, **21** (Ber8), with a chlorohexyl side chain at the 9-position, was seen to strongly interact with telomeric G-quadruplexes and could effectively induce acute cell growth arrest in cancer cells.

The inhibition of cancer cell growth by Ber8 was associated with apparent cell cycle arrest, cell senescence, and profound DNA damage at telomeric regions. Further mechanical studies revealed that Ber8 could not only increase the formation of endogenous telomeric G-quadruplexes in cancer cells but also delocalize TRF1 and POT1 from the telomere and induce telomere uncapping. In vivo experiments showed that **21** exhibited tumor-inhibition activity in SiHa xenograft tumors (Table 2) [96,97].

5.5. Other Alkaloid Derivatives

5.5.1. Quinazoline Derivatives

The design of derivatives **22–25** is derived from the 11-substituted quindoline derivative SYUIQ-5 (Figure 5) [98–100]. By retaining the 11-substituted amino side chain of SYUIQ-5 and opening the five-membered indole ring, a non-coplanar flexible structure was obtained. This molecule has an "imitative" tetracyclic aromatic system formed via intramolecular hydrogen bonds, which enables the adoption of moderately twisted and near-planar conformations of the aryl groups and allows the ligand to stack well on the G-quartet. Therefore, these derivatives effectively bind to telomeric G-quadruplexes but not to duplexes. The most effective derivative, **22**, has a K_D value of 3.14×10^{-7} M. NMR and molecular docking analyses indicate that hydrogen bonding, π-π stacking interactions, and electrostatic interactions may account for the overall interaction. Derivative **22** also induced distinct cell senescence and telomere shortening in HL-60 cells at micromolar concentrations. An effective *N*-(2-(quinazolin-2-yl) phenyl)benzamide (QPB) derivative, **23**, was subsequently obtained. These derivatives have strong induction abilities, leading to the conversion of hybrid telomeric G-quadruplexes to parallel G-quadruplexes. SAR analysis indicates that the presence of an additional

phenyl group and a chlorine substituent could greatly increase the stability and inducing ability of the derivative. Furthermore, a series of new 4-anilinoquinazoline derivatives were designed and synthetized; in these derivatives, the aromatic system of the quinazoline is expanded by introducing an anilino group at the 4-position of the quinazoline moiety to improve the G-quadruplex-binding activity and stability of the derivatives. The most effective derivative, **24**, has a K_D value of 2.1×10^{-7} M with the c-MYC G-quadruplex. Cellular studies showed that **24** significantly downregulated c-MYC gene transcription and expression in HeLa cells, presumably via the stabilization of the c-MYC G-quadruplex structure. In addition, real-time cell analyzer (RTCA) and colony formation assays indicated that **24** significantly inhibited HeLa cell proliferation but did not affect normal primary cultured mouse mesangial cells.
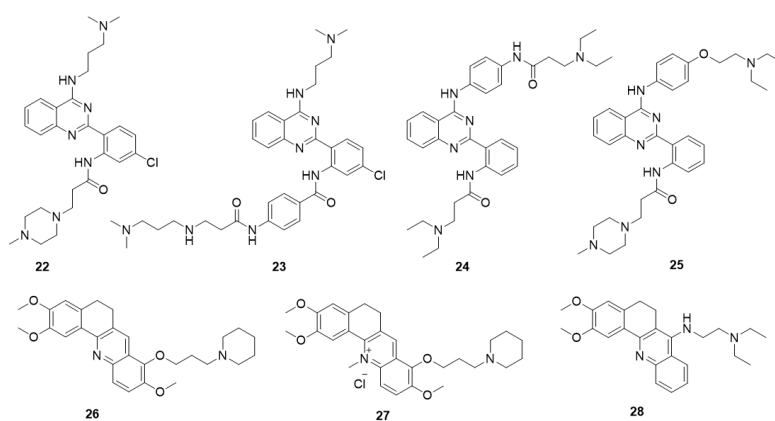
Figure 5. Structures of quinazoline derivatives and acridine derivatives.

An in-house small-molecule library screening by SPR identified a quinazoline derivative, **25**, which showed a significant and specific interaction with the 5′-UTR IRES-A RNA G-quadruplex of the hVEGF-A mRNA and destabilized the G-quadruplex structure [101]. Competition dialysis measurements were performed to verify the selectivity of the compounds. The IRES-A (WT) oligomer and several other oligomers, including an RNA hairpin, random RNA, CT DNA, IRES-MU2, flanking sequences of IRES, DNA G-quadruplexes (TBA, c-KIT 1, and c-MYC Pu27), and other RNA G-quadruplexes (ADAM10, TERRA, BCL-2, and NRAS), were placed in independent dialysis cassettes after the general annealing process. The results showed that derivative **25** exhibited strongest binding with the IRES-WT and weaker binding with other DNA and RNA structures. Further cellular experiments revealed that derivative **25** downregulated hVEGF-A translation and significantly impeded tumor-cell migration. In vivo experiments showed that **25** exhibited tumor inhibition in MCF-7 xenograft tumors (Table 2). These findings provided a new strategy for the regulation of hVEGF-A translation, in which small molecules interact with the G-quadruplex structure in the 5′ UTR.

5.5.2. Acridine Derivatives

Two series of 12-*N*-methylated and non-methylated 5,6-dihydrobenzo[*c*]acridine derivatives were designed by exploring the effect of the positive charge on berberine (Figure 5) [102,103]. The interactions of these derivatives with the c-MYC G-quadruplex were evaluated. Compared with the non-methylated derivative, **26**, the 12-*N*-methylated derivative, **27**, had stronger binding affinity and stabilizing ability toward the c-MYC G-quadruplex structure and could more effectively stack onto the G-quartet surface. All the derivatives had high selectivity for c-MYC G-quadruplex DNA over duplex DNA. The reverse transcription PCR (RT-PCR) assay showed that derivative **27** could downregulate transcription of the c-MYC gene in the Ramos cell line, containing an NHE III$_1$ element, but had no effect in the CA46 cell line, in which the NHE III$_1$ element had been removed. Recently, a series of 7-substituted 5,6-dihydrobenzo[*c*]acridine derivatives were synthesized as c-KIT

G-quadruplex-binding ligands. These derivatives presented higher stabilization ability and binding affinity toward G-quadruplex DNA in the c-KIT oncogene promoter compared with that toward duplex DNA. The most active derivative, **28**, significantly reduced the transcription of c-KIT and exhibited a concomitant reduction of c-KIT protein levels in K562 cells. In addition, **28** induced apoptosis via suppression of Bcl-2, upregulation of Bax and activation of caspase-3.

5.5.3. Multiaryl-Substituted Imidazole Derivatives

Multiaryl-substituted imidazole derivatives designed for G-quadruplex binding were first discovered by using a 3D-QSAR pharmacophore model to screen our in-house derivative database (Figure 6) [62]. Derivative **29** exhibited potent binding and stabilization activity as well as 8.7-fold higher selectivity towards telomeric G-quadruplex DNA over duplex DNA. Inspired by these promising results, our research group further optimized this class of ligands using CADD methods in parallel with organic synthesis. Derivative **30**, with a 1,8-naphthalimide instead of an *N*-methyl piperazine group, was found to specifically bind to and strongly stabilize telomeric multimeric G-quadruplexes by intercalating into the pocket between the two quadruplex units. Further cellular studies indicated that **30** could induce telomeric DNA damage and telomere dysfunction, eventually leading to cell cycle arrest, apoptosis and senescence in SiHa cancer cells [50]. Such behavior differed from that of traditional telomeric G-quadruplex ligands, providing new insights for the development of selective anticancer drugs targeting telomeric multimeric G-quadruplexes.

By replacing the *N*-methyl piperazine group with fluorophores, a series of small-molecular fluorescent probes were obtained. Derivative **31** exhibited distinct and specific fluorescence enhancement upon binding to parallel G-quadruplexes [104]. Derivative **32** greatly enhanced the detection limit of **31** for G-quadruplexes; the limit of detection (LOD) value of **32** for the G-quadruplex was up to 3 nM in solution and up to 5 ng in a gel matrix [105]. Derivative **33**, assembled with a triarylimidazole scaffold and a carboxyl side chain, was obtained as a positive hit by using in situ click chemistry, providing a method for identifying selective fluorescent probes for a specific topology of G-quadruplex nucleic acids. Derivative **34** showed great potential for the sensitive and selective detection of parallel G-quadruplexes [106]. A new tetra-arylimidazole probe, derivative **34**, exhibited significant and distinctive changes in both the absorption and fluorescence spectra in the presence of parallel G-quadruplexes but showed insignificant changes upon interaction with anti-parallel G-quadruplexes or non-quadruplex oligonucleotides. In view of this dual-output feature, **34** was further used to identify parallel G-quadruplexes from a large set of 314 oligonucleotides via a microplate reader, and thus, a high-throughput method for the characterization of parallel G-quadruplex topologies was established [107].
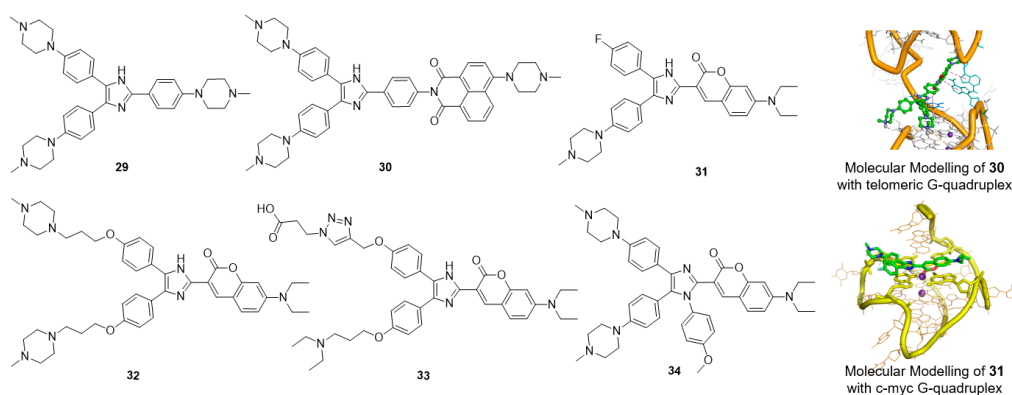
Figure 6. Multiaryl-substituted imidazole derivatives and binding mode with G-quadruplex.

6. Summary and Outlook

Natural alkaloids and their heterocyclic derivatives are valuable assets for drug discovery and development. The polymorphism and structural complexity of natural alkaloids and their derivatives make it possible to discover potential anticancer drugs with high selectivity for G-quadruplexes over duplex DNA. In this review, we compiled the published information regarding natural alkaloids and heterocyclic derivatives that have been identified by our group as G-quadruplex ligands. The crescent-shaped planar chromophore moieties preferentially bind to and stabilize G-quadruplexes, while flexible side chains can increase the selectivity for G-quadruplexes over duplex DNA. The direction of the side chain also greatly affects the binding activity; derivatives with the side chain located outside the crescent ring system always shows good activity.

Over the past decade, our research group has developed a pool of ligands with diverse structures based on natural alkaloids and heterocyclic derivatives, as potential anticancer agents that target G-quadruplex structures. The activity data is summarized in Tables 2 and 3. Although there is still a long way to go toward the improvement of cancer therapeutics, given the rapidly accumulating data on G-quadruplex structures and the biological functions and rapid development of G-quadruplex ligands, we are confident that a wealth of new derivatives that are less cytotoxic and have higher selectivity will emerge in the near future.

Table 3. Biological activity of alkaloid derivatives in the above sections.

| Compounds | Target G4 | Biochemical Activity | | | Cytotoxicity (IC$_{50}$) | Ref. |
		ΔT_m	K_D	^{tel}IC$_{50}$		
3	telomere	n.d.	n.d.	16 μM [b]	6.3 μM (SKOV-6)	[69]
4	telomere	13.0 °C	n.d.	6.4 μM [b]	n.d.	[70]
5	telomere	21.0 °C	n.d.	0.44 μM [b]	1.68 μM (SW620)	[73]
Quindoline **6**	telomere	14.0 °C	n.d.	0.31 μM [b]	1.21 μM (HL-60)	[74]
derivatives **7**	telomere	24.3 °C	0.19 μM (SPR)	5.5 μM [c]	45 μM (HL-60)	[75]
9	c-MYC	13.9 °C	1.1 μM (MST)	n.d.	0.19 μM (RAJI)	[77]
10	c-MYC	27.0 °C	1.3 μM (MST)	n.d.	4.7 μM (RAJI)	[78]
12	telomere	21.9 °C	0.1 μM (FIT)	7.8 μM [c]	29 μM (CA46)	[81–83]
Isaindigotone **13**	c-KIT	13.6 °C	0.6 μM (SPR)	n.d.	6.8 μM (HGC-27)	[81–83]
derivatives **14**	c-MYC [a]	n.d.	5.29 μM (SPR)	n.d.	13.1 μM (Hela)	[79]
15	c-MYC [a]	12.1 °C	17.0 μM (MST)	n.d.	16.0 μM (SiHA)	[79]
16	c-MYC [a]	0.5 °C	2.0 μM (MST)	n.d.	1.78 μM (SiHA)	[79]
18	telomere	23.4 °C	n.d.	n.d.	n.d.	[95]
Berberine **19**	telomere	28.2 °C	0.3 μM (FIT)	16 μM [b]	n.d.	[95]
derivatives **20**	telomere	25.0 °C	0.1 μM (FIT)	14 μM	n.d.	[95]
21	telomere	9.0 °C	14.8 μM	n.d.	1.7 μM (HL-60)	[95]
BRACO-19	telomere	27.5 °C	0.032 μM (SPR)	0.11 μM [c]	8 μM (21NT)	[19]
Telomestatin	telomere	n.d.	n.d.	0.005 μM [b]	0.8 μM (LAN1)	[108]

[a] target c-MYC G-quadruplex by interacting with NM23-H2; [b] telomerase inhibition by TRAP assay; [c] telomerase inhibition by TRAP-LIG assay.

Author Contributions: Tong Che has contributed to collect the data and write the manuscript Sections 4–6. Yu-Qing Wang and Zhou-Li Huang have contributed to revise the manuscript. Jia-Heng Tan and Zhi-Shu Huang have contributed to conception of the study. Shuo-Bin Chen has contributed to write the manuscript Sections 1–3 and revised the manuscript.

Conflicts of Interest: The authors declare no conflict of interest.

References

1. Smith, F.W.; Feigon, J. Quadruplex structure of Oxytricha telomeric DNA oligonucleotides. *Nature* **1992**, *356*, 164–168. [CrossRef] [PubMed]

2. Huppert, J.L.; Balasubramanian, S. Prevalence of quadruplexes in the human genome. *Nucleic Acids Res.* **2005**, *33*, 2908–2916. [CrossRef] [PubMed]

3. Eddy, J.; Maizels, N. Gene function correlates with potential for G4 DNA formation in the human genome. *Nucleic Acids Res.* **2006**, *34*, 3887–3896. [CrossRef] [PubMed]

4. Chambers, V.S.; Marsico, G.; Boutell, J.M.; Di Antonio, M.; Smith, G.P.; Balasubramanian, S. High-throughput sequencing of DNA G-quadruplex structures in the human genome. *Nat. Biotechnol.* **2015**, *33*, 877–881. [CrossRef] [PubMed]

5. Hansel-Hertsch, R.; Beraldi, D.; Lensing, S.V.; Marsico, G.; Zyner, K.; Parry, A.; Di Antonio, M.; Pike, J.; Kimura, H.; Narita, M.; et al. G-quadruplex structures mark human regulatory chromatin. *Nat. Genet.* **2016**, *48*, 1267–1272. [CrossRef] [PubMed]

6. Fedeles, B.I. G-quadruplex-forming promoter sequences enable transcriptional activation in response to oxidative stress. *Proc. Natl. Acad. Sci. USA* **2017**, *114*, 2788–2790. [CrossRef] [PubMed]

7. Kwok, C.K.; Marsico, G.; Sahakyan, A.B.; Chambers, V.S.; Balasubramanian, S. rG4-seq reveals widespread formation of G-quadruplex structures in the human transcriptome. *Nat. Methods* **2016**, *13*, 841–844. [CrossRef] [PubMed]

8. Wolfe, A.L.; Singh, K.; Zhong, Y.; Drewe, P.; Rajasekhar, V.K.; Sanghvi, V.R.; Mavrakis, K.J.; Jiang, M.; Roderick, J.E.; Van der Meulen, J.; et al. Rna G-quadruplexes cause eif4a-dependent oncogene translation in cancer. *Nature* **2014**, *513*, 65–70. [CrossRef] [PubMed]

9. Balasubramanian, S.; Hurley, L.H.; Neidle, S. Targeting G-quadruplexes in gene promoters: A novel anticancer strategy? *Nat. Rev. Drug Discov.* **2011**, *10*, 261–275. [CrossRef] [PubMed]

10. Phan, A.T.; Kuryavyi, V.; Gaw, H.Y.; Patel, D.J. Small-molecule interaction with a five-guanine-tract G-quadruplex structure from the human MYC promoter. *Nat. Chem. Biol.* **2005**, *1*, 234. [CrossRef]

11. Kim, M.Y.; Vankayalapati, H.; Shin-Ya, K.; Wierzba, K.; Hurley, L.H. Telomestatin, a potent telomerase inhibitor that interacts quite specifically with the human telomeric intramolecular G-quadruplex. *J. Am. Chem. Soc.* **2002**, *124*, 2098–2099. [CrossRef] [PubMed]

12. Chung, W.J.; Heddi, B.; Tera, M.; Iida, K.; Nagasawa, K.; Phan, A.T. Solution structure of an intramolecular (3 + 1) human telomeric G-quadruplex bound to a telomestatin derivative. *J. Am. Chem. Soc.* **2013**, *135*, 13495–13501. [CrossRef] [PubMed]

13. Rodriguez, R.; Miller, K.M.; Forment, J.V.; Bradshaw, C.R.; Nikan, M.; Britton, S.; Oelschlaegel, T.; Xhemalce, B.; Balasubramanian, S.; Jackson, S.P. Small-molecule-induced DNA damage identifies alternative DNA structures in human genes. *Nat. Chem. Biol.* **2012**, *8*, 301–310. [CrossRef] [PubMed]

14. Drygin, D.; Siddiqui-Jain, A.; O'Brien, S.; Schwaebe, M.; Lin, A.; Bliesath, J.; Ho, C.B.; Proffitt, C.; Trent, K.; Whitten, J.P.; et al. Anticancer activity of CX-3543: A direct inhibitor of rRNA biogenesis. *Cancer Res.* **2009**, *69*, 7653–7661. [CrossRef] [PubMed]

15. Huang, Z.S.S.; Zhou, X.; Tan, Z. Biological function of G-quadruplex nucleic acids and potential application in medicinal chemistry. *Curr. Top. Med. Chem.* **2015**, *15*, 1939. [CrossRef] [PubMed]

16. Rocca, R.; Moraca, F.; Costa, G.; Alcaro, S.; Distinto, S.; Maccioni, E.; Ortuso, F.; Artese, A.; Parrotta, L. Structure-based virtual screening of novel natural alkaloid derivatives as potential binders of *h-telo* and *c-myc* DNA G-quadruplex conformations. *Molecules* **2014**, *20*, 206–223. [CrossRef] [PubMed]

17. Ou, T.-M.; Lu, Y.-J.; Tan, J.-H.; Huang, Z.-S.; Wong, K.-Y.; Gu, L.-Q. G-quadruplexes: Targets in anticancer drug design. *ChemMedChem* **2008**, *3*, 690–713. [CrossRef] [PubMed]

18. Harrison, R.J.; Cuesta, J.; Chessari, G.; Read, M.A.; Basra, S.K.; Reszka, A.P.; Morrell, J.; Gowan, S.M.; Incles, C.M.; Tanious, F.A.; et al. Trisubstituted acridine derivatives as potent and selective telomerase inhibitors. *J. Med. Chem.* **2003**, *46*, 4463–4476. [CrossRef] [PubMed]

19. Moore, M.J.; Schultes, C.M.; Cuesta, J.; Cuenca, F.; Gunaratnam, M.; Tanious, F.A.; Wilson, W.D.; Neidle, S. Trisubstituted acridines as G-quadruplex telomere targeting agents. Effects of extensions of the 3,6- and 9-side chains on quadruplex binding, telomerase activity, and cell proliferation. *J. Med. Chem.* **2006**, *49*, 582–599. [CrossRef] [PubMed]

20. Muller, S.; Sanders, D.A.; Di Antonio, M.; Matsis, S.; Riou, J.F.; Rodriguez, R.; Balasubramanian, S. Pyridostatin analogues promote telomere dysfunction and long-term growth inhibition in human cancer cells. *Org. Biomol. Chem.* **2012**, *10*, 6537–6546. [CrossRef] [PubMed]

21. Gellert, M.; Lipsett, M.N.; Davies, D.R. Helix formation by guanylic acid. *Proc. Natl. Acad. Sci. USA* **1962**, *48*, 2013–2018. [CrossRef] [PubMed]

22. Phan, A.T.; Modi, Y.S.; Patel, D.J. Propeller-type parallel-stranded G-quadruplexes in the human c-myc promoter. *J. Am. Chem. Soc.* **2004**, *126*, 8710–8716. [CrossRef] [PubMed]

23. Hazel, P.; Parkinson, G.N.; Neidle, S. Topology variation and loop structural homology in crystal and simulated structures of a bimolecular DNA quadruplex. *J. Am. Chem. Soc.* **2006**, *128*, 5480–5487. [CrossRef] [PubMed]

24. Campbell, N.; Collie, G.W.; Neidle, S. Crystallography of DNA and RNA G-quadruplex nucleic acids and their ligand complexes. *Curr. Protoc. Nucleic Acid Chem.* **2012**. [CrossRef]

25. Matsugami, A.; Okuizumi, T.; Uesugi, S.; Katahira, M. Intramolecular higher order packing of parallel quadruplexes comprising a G:G:G:G tetrad and a G(:A):G(:A):G(:A):G heptad of GGA triplet repeat DNA. *J. Biol. Chem.* **2003**, *278*, 28147–28153. [CrossRef] [PubMed]

26. Neidle, S. The structures of quadruplex nucleic acids and their drug complexes. *Curr. Opin. Struct. Biol.* **2009**, *19*, 239–250. [CrossRef] [PubMed]

27. Collie, G.W.; Promontorio, R.; Hampel, S.M.; Micco, M.; Neidle, S.; Parkinson, G.N. Structural basis for telomeric G-quadruplex targeting by naphthalene diimide ligands. *J. Am. Chem. Soc.* **2012**, *134*, 2723–2731. [CrossRef] [PubMed]

28. Chung, W.J.; Heddi, B.; Hamon, F.; Teulade-Fichou, M.P.; Phan, A.T. Solution structure of a G-quadruplex bound to the bisquinolinium compound PHEN-DC(3). *Angew. Chem.* **2014**, *53*, 999–1002. [CrossRef] [PubMed]

29. Collie, G.W.; Sparapani, S.; Parkinson, G.N.; Neidle, S. Structural basis of telomeric RNA quadruplex–acridine ligand recognition. *J. Am. Chem. Soc.* **2011**, *133*, 2721–2728. [CrossRef] [PubMed]

30. Ma, D.-L.L.; Wang, M.; Lin, S.; Han, Q.-B.B.; Leung, C.-H.H. Recent Development of G-Quadruplex Probes for Cellular Imaging. *Curr. Top. Med. Chem.* **2015**, *15*, 1957–1963. [CrossRef] [PubMed]

31. Schaffitzel, C.; Berger, I.; Postberg, J.; Hanes, J.; Lipps, H.J.; Pluckthun, A. In vitro generated antibodies specific for telomeric guanine-quadruplex DNA react with Stylonychia lemnae macronuclei. *Proc. Natl. Acad. Sci. USA* **2001**, *98*, 8572–8577. [CrossRef] [PubMed]

32. Granotier, C.; Pennarun, G.; Riou, L.; Hoffschir, F.; Gauthier, L.R.; De Cian, A.; Gomez, D.; Mandine, E.; Riou, J.F.; Mergny, J.L.; et al. Preferential binding of a G-quadruplex ligand to human chromosome ends. *Nucleic Acids Res.* **2005**, *33*, 4182–4190. [CrossRef] [PubMed]

33. Chang, C.C.; Kuo, I.C.; Ling, I.F.; Chen, C.T.; Chen, H.C.; Lou, P.J.; Lin, J.J.; Chang, T.C. Detection of quadruplex DNA structures in human telomeres by a fluorescent carbazole derivative. *Anal. Chem.* **2004**, *76*, 4490–4494. [CrossRef] [PubMed]

34. Biffi, G.; Tannahill, D.; McCafferty, J.; Balasubramanian, S. Quantitative visualization of DNA G-quadruplex structures in human cells. *Nat. Chem.* **2013**, *5*, 182–186. [CrossRef] [PubMed]

35. Chang, C.C.; Chu, J.F.; Kao, F.J.; Chiu, Y.C.; Lou, P.J.; Chen, H.C.; Chang, T.C. Verification of antiparallel G-quadruplex structure in human telomeres by using two-photon excitation fluorescence lifetime imaging microscopy of the 3,6-Bis(1-methyl-4-vinylpyridinium)carbazole diiodide molecule. *Anal. Chem.* **2006**, *78*, 2810–2815. [CrossRef] [PubMed]

36. Yan, J.W.; Chen, S.B.; Liu, H.Y.; Ye, W.J.; Ou, T.M.; Tan, J.H.; Li, D.; Gu, L.Q.; Huang, Z.S. Development of a new colorimetric and red-emitting fluorescent dual probe for G-quadruplex nucleic acids. *Chem. Commun.* **2014**, *50*, 6927–6930. [CrossRef] [PubMed]

37. Chen, Y.; Yan, S.; Yuan, L.; Zhou, Y.; Song, Y.; Xiao, H.; Weng, X.; Zhou, X. Nonlinear optical dye TSQ1 as an efficiently selective fluorescent probe for G-quadruplex DNA. *Org. Chem. Front.* **2014**, *1*, 267. [CrossRef]

38. Vummidi, B.R.; Alzeer, J.; Luedtke, N.W. Fluorescent probes for G-quadruplex structures. *Chem. Biol. Chem.* **2013**, *14*, 540–558. [CrossRef] [PubMed]

39. Lu, Y.J.; Yan, S.C.; Chan, F.Y.; Zou, L.; Chung, W.H.; Wong, W.L.; Qiu, B.; Sun, N.; Chan, P.H.; Huang, Z.S.; et al. Benzothiazole-substituted benzofuroquinolinium dye: A selective switch-on fluorescent probe for G-quadruplex. *Chem. Commun.* **2011**, *47*, 4971–4973. [CrossRef] [PubMed]

40. Biffi, G.; Di Antonio, M.; Tannahill, D.; Balasubramanian, S. Visualization and selective chemical targeting of RNA G-quadruplex structures in the cytoplasm of human cells. *Nat. Chem.* **2014**, *6*, 75–80. [CrossRef] [PubMed]

41. Laguerre, A.; Hukezalie, K.; Winckler, P.; Katranji, F.; Chanteloup, G.; Pirrotta, M.; Perrier-Cornet, J.M.; Wong, J.M.; Monchaud, D. Visualization of RNA-quadruplexes in live cells. *J. Am. Chem. Soc.* **2015**, *137*, 8521–8525. [CrossRef] [PubMed]

42. Chen, S.-B.; Hu, M.-H.; Liu, G.-C.; Wang, J.; Ou, T.-M.; Gu, L.-Q.; Huang, Z.-S.; Tan, J.-H. Visualization of NRAS RNA G-quadruplex structures in cells with an engineered fluorogenic hybridization probe. *J. Am. Chem. Soc.* **2016**, *138*, 10382–10385. [CrossRef] [PubMed]

43. Blackburn, E.H. Structure and function of telomeres. *Nature* **1991**, *350*, 569–573. [CrossRef] [PubMed]

44. Chadeneau, C.; Hay, K.; Hirte, H.W.; Gallinger, S.; Bacchetti, S. Telomerase activity associated with acquisition of malignancy in human colorectal cancer. *Cancer Res.* **1995**, *55*, 2533–2536. [PubMed]

45. Phatak, P.; Cookson, J.C.; Dai, F.; Smith, V.; Gartenhaus, R.B.; Stevens, M.F.; Burger, A.M. Telomere uncapping by the G-quadruplex ligand RHPS4 inhibits clonogenic tumour cell growth in vitro and in vivo consistent with a cancer stem cell targeting mechanism. *Br. J. Cancer* **2007**, *96*, 1223–1233. [CrossRef] [PubMed]

46. Parkinson, G.N.; Lee, M.P.; Neidle, S. Crystal structure of parallel quadruplexes from human telomeric DNA. *Nature* **2002**, *417*, 876–880. [CrossRef] [PubMed]

47. Dai, J.; Carver, M.; Punchihewa, C.; Jones, R.A.; Yang, D. Structure of the Hybrid-2 type intramolecular human telomeric G-quadruplex in K+ solution: Insights into structure polymorphism of the human telomeric sequence. *Nucleic Acids Res.* **2007**, *35*, 4927–4940. [CrossRef] [PubMed]

48. Ambrus, A.; Chen, D.; Dai, J.; Bialis, T.; Jones, R.A.; Yang, D. Human telomeric sequence forms a hybrid-type intramolecular G-quadruplex structure with mixed parallel/antiparallel strands in potassium solution. *Nucleic Acids Res.* **2006**, *34*, 2723–2735. [CrossRef] [PubMed]

49. Abraham Punnoose, J.; Ma, Y.; Li, Y.; Sakuma, M.; Mandal, S.; Nagasawa, K.; Mao, H. Adaptive and specific recognition of telomeric G-quadruplexes via polyvalency induced unstacking of binding units. *J. Am. Chem. Soc.* **2017**, *139*, 7476–7484. [CrossRef] [PubMed]

50. Hu, M.-H.; Chen, S.-B.; Wang, B.; Ou, T.-M.; Gu, L.-Q.; Tan, J.-H.; Huang, Z.-S. Specific targeting of telomeric multimeric G-quadruplexes by a new triaryl-substituted imidazole. *Nucleic Acids Res.* **2016**, *45*, 1606–1618. [CrossRef] [PubMed]

51. Siddiqui-Jain, A.; Grand, C.L.; Bearss, D.J.; Hurley, L.H. Direct evidence for a G-quadruplex in a promoter region and its targeting with a small molecule to repress c-MYC transcription. *Proc. Natl. Acad. Sci. USA* **2002**, *99*, 11593–11598. [CrossRef] [PubMed]

52. Phan, A.T.; Kuryavyi, V.; Burge, S.; Neidle, S.; Patel, D.J. Structure of an unprecedented G-quadruplex scaffold in the human c-KIT promoter. *J. Am. Chem. Soc.* **2007**, *129*, 4386–4392. [CrossRef] [PubMed]

53. Dai, J.; Dexheimer, T.S.; Chen, D.; Carver, M.; Ambrus, A.; Jones, R.A.; Yang, D. An intramolecular G-quadruplex structure with mixed parallel/antiparallel g-strands formed in the human BCL-2 promoter region in solution. *J. Am. Chem. Soc.* **2006**, *128*, 1096–1098. [CrossRef] [PubMed]

54. Cogoi, S.; Xodo, L.E. G-quadruplex formation within the promoter of the KRAS proto-oncogene and its effect on transcription. *Nucleic Acids Res.* **2006**, *34*, 2536–2549. [CrossRef] [PubMed]

55. Sun, D.; Guo, K.; Rusche, J.J.; Hurley, L.H. Facilitation of a structural transition in the polypurine/polypyrimidine tract within the proximal promoter region of the human VEGF gene by the presence of potassium and G-quadruplex-interactive agents. *Nucleic Acids Res.* **2005**, *33*, 6070–6080. [CrossRef] [PubMed]

56. Xu, Y.; Sugiyama, H. Formation of the G-quadruplex and i-motif structures in retinoblastoma susceptibility genes (RB). *Nucleic Acids Res.* **2006**, *34*, 949–954. [CrossRef] [PubMed]

57. Qin, Y.; Rezler, E.M.; Gokhale, V.; Sun, D.; Hurley, L.H. Characterization of the G-quadruplexes in the duplex nuclease hypersensitive element of the PDGF-A promoter and modulation of PDGF-A promoter activity by TMPyP4. *Nucleic Acids Res.* **2007**, *35*, 7698–7713. [CrossRef] [PubMed]

58. Gomez, D.; Lemarteleur, T.; Lacroix, L.; Mailliet, P.; Mergny, J.L.; Riou, J.F. Telomerase downregulation induced by the G-quadruplex ligand 12459 in A549 cells is mediated by hTERT RNA alternative splicing. *Nucleic Acids Res.* **2004**, *32*, 371–379. [CrossRef] [PubMed]

59. Hanahan, D.; Weinberg, R.A. The hallmarks of cancer. *Cell* **2000**, *100*, 57–70. [CrossRef]

60. Soucek, L.; Whitfield, J.; Martins, C.P.; Finch, A.J.; Murphy, D.J.; Sodir, N.M.; Karnezis, A.N.; Swigart, L.B.; Nasi, S.; Evan, G.I. Modelling MYC inhibition as a cancer therapy. *Nature* **2008**, *455*, 679–683. [CrossRef] [PubMed]

61. Guo, J.U.; Bartel, D.P. RNA G-quadruplexes are globally unfolded in eukaryotic cells and depleted in bacteria. *Science* **2016**, *353*, aaf5371. [CrossRef] [PubMed]

62. Chen, S.B.; Tan, J.H.; Ou, T.M.; Huang, S.L.; An, L.K.; Luo, H.B.; Li, D.; Gu, L.Q.; Huang, Z.S. Pharmacophore-based discovery of triaryl-substituted imidazole as new telomeric G-quadruplex ligand. *Bioorg. Med. Chem. Lett.* **2011**, *21*, 1004–1009. [CrossRef] [PubMed]

63. Cosconati, S.; Marinelli, L.; Trotta, R.; Virno, A.; Mayol, L.; Novellino, E.; Olson, A.J.; Randazzo, A. Tandem application of virtual screening and NMR experiments in the discovery of brand new DNA quadruplex groove binders. *J. Am. Chem. Soc.* **2009**, *131*, 16336–16337. [CrossRef] [PubMed]

64. Monchaud, D.; Allain, C.; Teulade-Fichou, M.P. Development of a fluorescent intercalator displacement assay (G4-FID) for establishing quadruplex-DNA affinity and selectivity of putative ligands. *Bioorg. Med. Chem. Lett.* **2006**, *16*, 4842–4845. [CrossRef] [PubMed]

65. Zhou, Q.; Li, L.; Xiang, J.; Sun, H.; Tang, Y. Fast screening and structural elucidation of G-quadruplex ligands from a mixture via G-quadruplex recognition and NMR methods. *Biochimie* **2009**, *91*, 304–308. [CrossRef] [PubMed]

66. Renciuk, D.; Zhou, J.; Beaurepaire, L.; Guedin, A.; Bourdoncle, A.; Mergny, J.L. A fret-based screening assay for nucleic acid ligands. *Methods* **2012**, *57*, 122–128. [CrossRef] [PubMed]

67. Redman, J.E. Surface plasmon resonance for probing quadruplex folding and interactions with proteins and small molecules. *Methods* **2007**, *43*, 302–312. [CrossRef] [PubMed]

68. Musumeci, D.; Amato, J.; Zizza, P.; Platella, C.; Cosconati, S.; Cingolani, C.; Biroccio, A.; Novellino, E.; Randazzo, A.; Giancola, C.; et al. Tandem application of ligand-based virtual screening and G4-OAS assay to identify novel G-quadruplex-targeting chemotypes. *Biochim. Biophys. Acta* **2017**, *1861*, 1341–1352. [CrossRef] [PubMed]

69. Dwuma-Badu, D.; Ayim, J.S.; Fiagbe, N.I.; Knapp, J.E.; Schiff, P.L., Jr.; Slatkin, D.J. Constituents of West African medicinal plants XX: Quindoline from cryptolepis sanguinolenta. *J. Pharm. Sci.* **1978**, *67*, 433–434. [CrossRef] [PubMed]

70. Caprio, V.; Guyen, B.; Opoku-Boahen, Y.; Mann, J.; Gowan, S.M.; Kelland, L.M.; Read, M.A.; Neidle, S. A novel inhibitor of human telomerase derived from 10H-indolo[3,2-*b*]quinoline. *Bioorg. Med. Chem. Lett.* **2000**, *10*, 2063–2066. [CrossRef]

71. Zhou, J.-L.; Lu, Y.-J.; Ou, T.-M.; Zhou, J.-M.; Huang, Z.-S.; Zhu, X.-F.; Du, C.-J.; Bu, X.-Z.; Ma, L.; Gu, L.-Q.; et al. Synthesis and evaluation of quindoline derivatives as G-quadruplex inducing and stabilizing ligands and potential inhibitors of telomerase. *J. Med. Chem.* **2005**, *48*, 7315–7321. [CrossRef] [PubMed]

72. Ou, T.-M.; Lu, Y.-J.; Zhang, C.; Huang, Z.-S.; Wang, X.-D.; Tan, J.-H.; Chen, Y.; Ma, D.-L.; Wong, K.-Y.; Tang, J.-C.; et al. Stabilization of G-quadruplex DNA and down-regulation of oncogene c-myc by quindoline derivatives. *J. Med. Chem.* **2007**, *50*, 1465–1474. [CrossRef] [PubMed]

73. Zhou, J.-M.; Zhu, X.-F.; Lu, Y.-J.; Deng, R.; Huang, Z.-S.; Mei, Y.-P.; Wang, Y.; Huang, W.-L.; Liu, Z.-C.; Gu, L.-Q.; et al. Senescence and telomere shortening induced by novel potent G-quadruplex interactive agents, quindoline derivatives, in human cancer cell lines. *Oncogene* **2006**, *25*, 503–511. [CrossRef] [PubMed]

74. Lu, Y.-J.; Ou, T.-M.; Tan, J.-H.; Hou, J.-Q.; Shao, W.-Y.; Peng, D.; Sun, N.; Wang, X.-D.; Wu, W.-B.; Bu, X.-Z.; et al. 5-*N*-methylated quindoline derivatives as telomeric G-quadruplex stabilizing ligands: Effects of 5-*N* positive charge on quadruplex binding affinity and cell proliferation. *J. Med. Chem.* **2008**, *51*, 6381–6392. [CrossRef] [PubMed]

75. Long, Y.; Li, Z.; Tan, J.-H.; Ou, T.-M.; Li, D.; Gu, L.-Q.; Huang, Z.-S. Benzofuroquinoline derivatives had remarkable improvement of their selectivity for telomeric G-quadruplex DNA over duplex DNA upon introduction of peptidyl group. *Bioconjug. Chem.* **2012**, *23*, 1821–1831. [CrossRef] [PubMed]

76. Dai, J.; Carver, M.; Hurley, L.H.; Yang, D. Solution structure of a 2:1 quindoline-c-MYC G-quadruplex: Insights into G-quadruplex-interactive small molecule drug design. *J. Am. Chem. Soc.* **2011**, *133*, 17673–17680. [CrossRef] [PubMed]

77. Zeng, D.-Y.; Kuang, G.-T.; Wang, S.-K.; Peng, W.; Lin, S.-L.; Zhang, Q.; Su, X.-X.; Hu, M.-H.; Wang, H.; Tan, J.-H.; et al. Discovery of novel 11-triazole substituted benzofuro[3,2-*b*]quinolone derivatives as c-myc G-quadruplex specific stabilizers via click chemistry. *J. Med. Chem.* **2017**, *60*, 5407–5423. [CrossRef] [PubMed]

78. Liu, H.-Y.; Chen, A.-C.; Yin, Q.-K.; Li, Z.; Huang, S.-M.; Du, G.; He, J.-H.; Zan, L.-P.; Wang, S.-K.; Xu, Y.-H.; et al. New disubstituted quindoline derivatives inhibiting burkitt's lymphoma cell proliferation by impeding c-MYC transcription. *J. Med. Chem.* **2017**, *60*, 5438–5454. [CrossRef] [PubMed]

79. Shan, C.; Lin, J.; Hou, J.-Q.; Liu, H.-Y.; Chen, S.-B.; Chen, A.-C.; Ou, T.-M.; Tan, J.-H.; Li, D.; Gu, L.-Q.; et al. Chemical intervention of the NM23-H2 transcriptional programme on c-MYC via a novel small molecule. *Nucleic Acids Res.* **2015**, *43*, 6677–6691. [CrossRef] [PubMed]

80. Wu, X.; Qin, G.; Cheung, K.K.; Cheng, K.F. New alkaloids from isatis indigotica. *Tetrahedron* **1997**, *53*, 13323–13328. [CrossRef]

81. Tan, J.-H.; Ou, T.-M.; Hou, J.-Q.; Lu, Y.-J.; Huang, S.-L.; Luo, H.-B.; Wu, J.-Y.; Huang, Z.-S.; Wong, K.-Y.; Gu, L.-Q. Isaindigotone derivatives: A new class of highly selective ligands for telomeric G-quadruplex DNA. *J. Med. Chem.* **2009**, *52*, 2825–2835. [CrossRef] [PubMed]

82. Hou, J.-Q.; Tan, J.-H.; Wang, X.-X.; Chen, S.-B.; Huang, S.-Y.; Yan, J.-W.; Chen, S.-H.; Ou, T.-M.; Luo, H.-B.; Li, D.; et al. Impact of planarity of unfused aromatic molecules on G-quadruplex binding: Learning from isaindigotone derivatives. *Org. Biomol. Chem.* **2011**, *9*, 6422–6436. [CrossRef] [PubMed]

83. Wang, X.; Zhou, C.-X.; Yan, J.-W.; Hou, J.-Q.; Chen, S.-B.; Ou, T.-M.; Gu, L.-Q.; Huang, Z.-S.; Tan, J.-H. Synthesis and evaluation of quinazolone derivatives as a new class of c-KIT G-quadruplex binding ligands. *ACS Med. Chem. Lett.* **2013**, *4*, 909–914. [CrossRef] [PubMed]

84. Vy Thi Le, T.; Han, S.; Chae, J.; Park, H.J. G-quadruplex binding ligands: From naturally occurring to rationally designed molecules. *Curr. Pharm. Des.* **2012**, *18*, 1948–1972. [CrossRef] [PubMed]

85. Muller, S.; Rodriguez, R. G-quadruplex interacting small molecules and drugs: From bench toward bedside. *Expert Rev. Clin. Pharmacol.* **2014**, *7*, 663–679. [CrossRef] [PubMed]

86. Grande, V.; Doria, F.; Freccero, M.; Wurthner, F. An aggregating amphiphilic squaraine: A light-up probe that discriminates parallel G-quadruplexes. *Angew. Chem.* **2017**, *56*, 7520–7524. [CrossRef] [PubMed]

87. Laguerre, A.; Stefan, L.; Larrouy, M.; Genest, D.; Novotna, J.; Pirrotta, M.; Monchaud, D. A twice-as-smart synthetic g-quartet: PyroTASQ is both a smart quadruplex ligand and a smart fluorescent probe. *J. Am. Chem. Soc.* **2014**, *136*, 12406–12414. [CrossRef] [PubMed]

88. Thakur, R.K.; Kumar, P.; Halder, K.; Verma, A.; Kar, A.; Parent, J.L.; Basundra, R.; Kumar, A.; Chowdhury, S. Metastases suppressor NM23-H2 interaction with G-quadruplex DNA within c-myc promoter nuclease hypersensitive element induces c-MYC expression. *Nucleic Acids Res.* **2009**, *37*, 172–183. [CrossRef] [PubMed]

89. Shan, C.; Yan, J.-W.; Wang, Y.-Q.; Che, T.; Huang, Z.-L.; Chen, A.-C.; Yao, P.-F.; Tan, J.-H.; Li, D.; Ou, T.-M.; et al. Design, synthesis, and evaluation of isaindigotone derivatives to downregulate c-myc transcription via disrupting the interaction of NM23-H2 with G-quadruplex. *J. Med. Chem.* **2017**, *60*, 1292–1308. [CrossRef] [PubMed]

90. Wang, Y.-Q.; Huang, Z.-L.; Chen, S.-B.; Wang, C.-X.; Shan, C.; Yin, Q.-K.; Ou, T.-M.; Li, D.; Gu, L.-Q.; Tan, J.-H.; et al. Design, synthesis, and evaluation of new selective NM23-H2 binders as c-MYC transcription inhibitors via disruption of the NM23-H2/G-quadruplex interaction. *J. Med. Chem.* **2017**, *60*, 6924–6941. [CrossRef] [PubMed]

91. Naasani, I.; Seimiya, H.; Yamori, T.; Tsuruo, T. FJ5002: A potent telomerase inhibitor identified by exploiting the disease-oriented screening program with COMPARE analysis. *Cancer Res.* **1999**, *59*, 4004–4011. [PubMed]

92. Zhang, W.-J.; Ou, T.-M.; Lu, Y.-J.; Huang, Y.-Y.; Wu, W.-B.; Huang, Z.-S.; Zhou, J.-L.; Wong, K.-Y.; Gu, L.-Q. 9-substituted berberine derivatives as G-quadruplex stabilizing ligands in telomeric DNA. *Bioorg. Med. Chem.* **2007**, *15*, 5493–5501. [CrossRef] [PubMed]

93. Ma, Y.; Ou, T.-M.; Hou, J.-Q.; Lu, Y.-J.; Tan, J.-H.; Gu, L.-Q.; Huang, Z.-S. 9-*N*-substituted berberine derivatives: Stabilization of G-quadruplex DNA and down-regulation of oncogene c-myc. *Bioorg. Med. Chem.* **2008**, *16*, 7582–7591. [CrossRef] [PubMed]

94. Ma, Y.; Ou, T.-M.; Tan, J.-H.; Hou, J.-Q.; Huang, S.-L.; Gu, L.-Q.; Huang, Z.-S. Synthesis and evaluation of 9-*O*-substituted berberine derivatives containing aza-aromatic terminal group as highly selective telomeric G-quadruplex stabilizing ligands. *Bioorg. Med. Chem. Lett.* **2009**, *19*, 3414–3417. [CrossRef] [PubMed]

95. Bazzicalupi, C.; Ferraroni, M.; Bilia, A.R.; Scheggi, F.; Gratteri, P. The crystal structure of human telomeric DNA complexed with berberine: An interesting case of stacked ligand to g-tetrad ratio higher than 1:1. *Nucleic Acids Res.* **2013**, *41*, 632–638. [CrossRef] [PubMed]

96. Xiao, N.; Chen, S.; Ma, Y.; Qiu, J.; Tan, J.-H.; Ou, T.-M.; Gu, L.-Q.; Huang, Z.-S.; Li, D. Interaction of berberine derivative with protein POT1 affect telomere function in cancer cells. *Biochem. Biophys. Res. Commun.* **2012**, *419*, 567–572. [CrossRef] [PubMed]

97. Xiong, Y.-X.; Su, H.-F.; Lv, P.; Ma, Y.; Wang, S.-K.; Miao, H.; Liu, H.-Y.; Tan, J.-H.; Ou, T.-M.; Gu, L.-Q.; et al. A newly identified berberine derivative induces cancer cell senescence by stabilizing endogenous G-quadruplexes and sparking a DNA damage response at the telomere region. *Oncotarget* **2015**, *6*, 35625–35635. [CrossRef] [PubMed]

98. Li, Z.; Tan, J.-H.; He, J.-H.; Long, Y.; Ou, T.-M.; Li, D.; Gu, L.-Q.; Huang, Z.-S. Disubstituted quinazoline derivatives as a new type of highly selective ligands for telomeric G-quadruplex DNA. *Eur. J. Med. Chem.* **2012**, *47*, 299–311. [CrossRef] [PubMed]

99. He, J.-H.; Liu, H.-Y.; Li, Z.; Tan, J.-H.; Ou, T.-M.; Huang, S.-L.; An, L.-K.; Li, D.; Gu, L.-Q.; Huang, Z.-S. New quinazoline derivatives for telomeric G-quadruplex DNA: Effects of an added phenyl group on quadruplex binding ability. *Eur. J. Med. Chem.* **2013**, *63*, 1–13. [CrossRef] [PubMed]

100. Jiang, Y.; Chen, A.C.; Kuang, G.T.; Wang, S.K.; Ou, T.M.; Tan, J.H.; Li, D.; Huang, Z.S. Design, synthesis and biological evaluation of 4-anilinoquinazoline derivatives as new c-myc G-quadruplex ligands. *Eur. J. Med. Chem.* **2016**, *122*, 264–279. [CrossRef] [PubMed]

101. Wang, S.-K.; Wu, Y.; Wang, X.-Q.; Kuang, G.-T.; Zhang, Q.; Lin, S.-L.; Liu, H.-Y.; Tan, J.-H.; Huang, Z.-S.; Ou, T.-M. Discovery of small molecules for repressing cap-independent translation of human vascular endothelial growth factor (hVEGF) as novel antitumor agents. *J. Med. Chem.* **2017**, *60*, 5306–5319. [CrossRef] [PubMed]

102. Liao, S.-R.; Zhou, C.-X.; Wu, W.-B.; Ou, T.-M.; Tan, J.-H.; Li, D.; Gu, L.-Q.; Huang, Z.-S. 12-*N*-Methylated 5,6-dihydrobenzo[c]acridine derivatives: A new class of highly selective ligands for c-myc G-quadruplex DNA. *Eur. J. Med. Chem.* **2012**, *53*, 52–63. [CrossRef] [PubMed]

103. Guo, Q.L.; Su, H.F.; Wang, N.; Liao, S.R.; Lu, Y.T.; Ou, T.M.; Tan, J.H.; Li, D.; Huang, Z.S. Synthesis and evaluation of 7-substituted-5,6-dihydrobenzo[*c*]acridine derivatives as new c-KIT promoter G-quadruplex binding ligands. *Eur. J. Med. Chem.* **2017**, *130*, 458–471. [CrossRef] [PubMed]

104. Chen, S.-B.; Wu, W.-B.; Hu, M.-H.; Ou, T.-M.; Gu, L.-Q.; Tan, J.-H.; Huang, Z.-S. Discovery of a new fluorescent light-up probe specific to parallel G-quadruplexes. *Chem. Commun.* **2014**, *50*, 12173–12176. [CrossRef] [PubMed]

105. Hu, M.-H.; Chen, S.-B.; Guo, R.-J.; Ou, T.-M.; Huang, Z.-S.; Tan, J.-H. Development of a highly sensitive fluorescent light-up probe for G-quadruplexes. *Analyst* **2015**, *140*, 4616–4625. [CrossRef] [PubMed]

106. Hu, M.-H.; Chen, X.; Chen, S.-B.; Ou, T.-M.; Yao, M.; Gu, L.-Q.; Huang, Z.-S.; Tan, J.-H. A new application of click chemistry in situ: Development of fluorescent probe for specific G-quadruplex topology. *Sci. Rep.* **2015**, *5*, 17202. [CrossRef] [PubMed]

107. Hu, M.-H.; Chen, S.-B.; Wang, Y.-Q.; Zeng, Y.-M.; Ou, T.-M.; Li, D.; Gu, L.-Q.; Huang, Z.-S.; Tan, J.-H. Accurate high-throughput identification of parallel G-quadruplex topology by a new tetraaryl-substituted imidazole. *Biosens. Bioelectron.* **2016**, *83*, 77–84. [CrossRef] [PubMed]

108. Shin-ya, K.; Wierzba, K.; Matsuo, K.; Ohtani, T.; Yamada, Y.; Furihata, K.; Hayakawa, Y.; Seto, H. Telomestatin, a novel telomerase inhibitor from Streptomyces anulatus. *J. Am. Chem. Soc.* **2001**, *123*, 1262–1263. [CrossRef] [PubMed]

Sample Availability: Samples of the compounds are available from the authors.